

Sources of dissolved organic matter during storm and inter-storm conditions in a lowland headwater catchment: constraints from high-frequency molecular data

L. Jeanneau¹, M. Denis¹, A-C. Pierson-Wickmann¹, G. Gruau¹, T. Lambert^{1,*} and P. Petitjean¹

[1]{UMR 6118 Géosciences Rennes, Université de Rennes 1/CNRS, 35042 Rennes, France}

[*]{now at: University of Liège, Institut de Physique (B5), B-4000 Sart Tilman}

Correspondence to: L. Jeanneau (laurent.jeanneau@univ-rennes1.fr)

Abstract

The transfer of dissolved organic matter (DOM) at soil-river interfaces controls the biogeochemistry of micropollutants and the equilibrium between continental and oceanic C reservoirs. Understanding the mechanisms controlling this transfer is fundamental to ecology and geochemistry. DOM delivery to streams during storms is assumed to come from the flushing of pre-existing soil DOM reservoirs mobilized by the modification of water flow paths. We tested this hypothesis by investigating the evolution of the composition of stream DOM during inter-storm conditions and five storm events monitored with a high-frequency sampling. The composition of DOM was analyzed using thermally assisted hydrolysis and methylation (THM) using tetramethylammonium hydroxide (TMAH) coupled to a gas chromatograph and mass spectrometer. In inter-storm conditions, stream DOM is derived from the flushing of soil DOM, while during storm events, the modification of the distribution of chemical biomarkers allows the identification of three additional mechanisms. The first one corresponds to the destabilization of microbial biofilms due to the increase in water velocity resulting in the fleeting export of a microbial pool. The second mechanism corresponds to the erosion of soils and river banks leading to a partition of organic matter between particles and dissolved phase. The third mechanism is linked to the increase in water velocity in soils that could induce the erosion of macropore walls leading to an in-soil partitioning between soil microparticles and dissolved phase. The contribution of this in-soil erosive process would be

linked to the magnitude of the hydraulic gradient following the rise of water table and could persist after the recession, which could explain why the return to inter-storm composition of DOM does not follow the same temporal scheme as the discharge. Those results are of main importance to understand the transfer of nutrients and micropollutants at the soil-river interfaces during the hot moments that are storm events.

1 Introduction

The transfer of dissolved organic matter (DOM) across soil-river interfaces is a globally relevant carbon flux (Cole et al., 2007) and a major control on the biogeochemistry of micropollutants (Corapcioglu and Jiang, 1993; Raymond et al., 2013). While the mechanisms governing this transfer have clear ecological, societal and geochemical implications, key unknowns persist concerning the production and transfer of DOM across terrestrial-aquatic interfaces (Kicklighter et al., 2013; Lambert et al., 2014). Understanding DOM dynamics in headwater catchments is particularly important because over 90% of stream length occurs in small catchments (Bishop et al., 2008) and DOM yield per square meter is highest in headwaters (Ågren et al., 2007), resulting in a large proportion of river DOM ultimately coming from headwater catchment soils (Billett et al., 2006; Morel et al., 2009). Organic matter sources are typically abundant in headwater catchment soil, meaning that DOM flux depends primarily on water flow path (McDonnell, 2003; Morel et al., 2009), which changes at seasonal and event scales in response to hydroclimatic conditions (Hinton et al., 1998). Because storm events connect a larger portion of the landscape with surface waters, more than 60% of annual dissolved organic carbon (DOC; the parameter commonly used to quantify DOM concentration) load can occur during storm events (Morel et al., 2009). DOC concentration typically increases during storm events as elevated water table and enhanced near-surface flow cause leaching of DOM-rich soil horizons (Maurice et al., 2002; McGlynn and McDonnell, 2003).

The shift in flow paths during storm events can also cause changes in DOM composition and biodegradability (McLaughlin and Kaplan, 2013). Low frequency spectroscopic measurements of UV-absorbance and fluorescence suggested that DOM aromaticity increases during storm events, potentially due to mobilization of aromatic DOM from surface soil horizons (Hood et al., 2006; Maurice et al., 2002). However high frequency spectroscopic measurements have shown that concentration and composition are not always linked and that

1 compositional differences in DOM can persist long after concentration returns to pre-event
2 levels (Austnes et al., 2010; Knorr, 2013; Saraceno et al., 2009; Yang et al., 2013). This shift
3 in DOM signature has been attributed to in-stream production of fluorescing DOM (Austnes
4 et al., 2010) or sustained hydrologic contribution from surface soil horizons after the return to
5 low-flow conditions (Strohmeier et al., 2013).

6 Analysis of the molecular composition of DOM during low and high-flow conditions is
7 considerably less common than spectroscopic data due to analytical cost and complexity.
8 However, low frequency lignin phenol data indicate that less-degraded lignins are mobilized
9 during storm events potentially due to the mobilization of particles by erosion combined with
10 partitioning of the lignin compounds between the solid and dissolved phase (Dalzell et al.,
11 2005; Hernes et al., 2008). This partitioning process could be linked to in-stream production
12 of fluorescing DOM (Austnes et al., 2010). However because molecular data are typically
13 collected using low frequency water sampling strategies (one sample per storm event), it is
14 not possible to evaluate the persistence of shifts in DOM aromatic fingerprint after storm
15 events.

16 These asymmetrical shifts in DOM composition during and after storm events suggest that in
17 addition to changing flow path and DOM transport, storm events alter mechanisms of DOM
18 production or processing. To test this hypothesis, we collected high-frequency molecular data
19 during five successive storm events and we compared them with background information on
20 the molecular composition of soil organic matter (SOM), soil DOM and inter-storm river
21 DOM in a lowland headwater catchment in Brittany, France.

22 Among the different techniques available to study the molecular composition of DOM,
23 thermally assisted hydrolysis and methylation (THM) using tetramethylammonium hydroxide
24 (TMAH) coupled to a gas chromatograph and mass spectrometer (THM-GC-MS) seems to be
25 particularly suitable. This technique can be used to simultaneously analyze phenol markers
26 from lignins and tannins (LIG-TAN), carbohydrates (CAR) and fatty acids (FA) (Grasset et
27 al., 2009). LIG-TAN are commonly used to monitor the input of terrestrially-derived OM to
28 oceans (Hedges and Parker, 1976) and their investigation has led to the partitioning process
29 invoked for lignin compounds during storm events (Dalzell et al., 2005; Hernes et al., 2008).
30 Analysis of CAR can differentiate between plant-derived and microbial inputs (Rumpel and
31 Dignac, 2006) since the distribution of non-cellulosic monosaccharides is dominated by
32 pentose (C5) for plant-derived inputs and by hexose (C6) and deoxyhexose (deoxyC6) for

microbial inputs. Similar to CAR, the distribution of FA differs in plant-derived and microbial inputs (Cranwell, 1974; Eglinton and Hamilton, 1967; Lucas García et al., 2001; Matsuda and Koyama, 1977). The combination of those markers allows the investigation of the balance between microbial and plant-derived markers differentiating between soil DOM from organic-rich, characterized by high proportion of plant-derived markers, and organic-poor horizons, characterized by high proportion of microbial markers, in a wetland submitted to fluctuating water-table level and being correlated with the specific UV absorbance (SUVA) at 254 nm (Jeanneau et al., 2014).

Two main questions motivated our work. First, how does the molecular composition of DOM vary during and between storm events? Second, what new insights can molecular data provide on the sources and transfer mechanisms of DOM during storms?

2 Materials and methods

2.1 Site description

We collected samples from the outlet of the Kervidy-Naizin catchment, a 4.9 km² lowland catchment located in central Brittany in western France (Figure 1). The catchment is a part of a long-term monitoring research program aimed at understanding the impact of agricultural intensification and climate change on hydrologic processes and water quality. Numerous hydrological and biogeochemical studies have already been undertaken at this site (Lambert et al., 2013 and references therein) including investigating the effect of storm events on hydrology (Aubert et al., 2013; Durand and Juan Torres, 1996; Morel et al., 2009) and DOM sources and transfer processes (Lambert et al., 2011, 2013, 2014; Morel et al., 2009).

The Kervidy-Naizin catchment has a temperate oceanic climate with mean annual temperature and precipitation (1993-2011) of 10.7°C and 814 mm, respectively. Rainfall events rarely exceed 20 mm per day, and 80% of rainfall events have an intensity of less than 4 mm per hour. The stream is ephemeral and often does not flow from the end of August to October due to the small volume of water stored in the bedrock. High-flow generally lasts from December to April, with maximum discharges in February and March. Catchment topography is gentle, with hillslope gradients of less than 5% and elevation ranging from 93 to 135 m above sea level. Soil depth ranges from 0.5 to 1.5 m with soils classified as silty loams, specifically Stagnic fluvisols (IUSS Working Group WRB, 2006) developed from alluvial material and

Brioverian schist. The aquifer in the catchment consists of unconsolidated weathered bedrock, underlain by a locally fractured but generally impermeable unmodified bedrock.

The hydrologic regime is characterized by three distinct periods (Lambert et al., 2013; Molenat et al., 2008). First, in the autumn, the water table reaches the riparian zone but remains below the surface in the upland domain (period A). Second, as precipitation increases through the winter, the water table rises in the upland domain, connecting upland and riparian areas hydrologically and consequently increasing upland groundwater flow towards the riparian zone (period B). Third, in late spring and summer, upland groundwater flow decreases progressively resulting in a gradual air-drying of wetland soils (period C).

The extent of interaction between the organic-rich soils and groundwater fluctuates strongly with hydroclimatic conditions within and between years. During dry hydrologic years, it may be restricted to riparian or wetland areas, which represent less than 5% of the total catchment area. Conversely, during wet hydrological years, water table may be in contact with 20% of the total catchment surface area (Crave and Gascuel-Odoux, 1997).

2.2 Previous data

2.2.1 Molecular data on SOM and soil DOM

The molecular composition of SOM and the spatio-temporal variation of the molecular composition of soil DOM were investigated in the central, most widespread wetland zone of the catchment (so-called Mercy wetland) during the hydrologic year 2010-2011 (Jeanneau et al., 2014). Concerning SOM, the proportion of LIG-TAN, CAR and FA were 16, 29 and 55 % and 4, 3 and 93 % in the organo-mineral and mineral horizons, respectively. The deoxyC6/C5 ratio was 0.4 and 0.2 in the organo-mineral and mineral horizons, respectively and the proportion of plant-derived markers was 88 and 71 % in the organo-mineral and mineral horizons, respectively.

During hydrologic period B, when the five studied storm events were sampled, there was a clear differentiation between surface (10 cm) and deep (50 cm) soil DOM. In the surface horizons, the proportion of plant-derived markers remained higher than 70% with a mean value of 0.8 ± 0.1 (standard deviation) for the ratio deoxyC6/C5. While in the deep horizon,

1 this proportion was lower than 30% with a mean value of 1.3 ± 0.2 (standard deviation) for the
2 ratio deoxyC6/C5.

3 **2.2.2 Previous data on river samples**

4 The intra-storm variability of $\delta^{13}\text{C}$ values ranged between the values recorded in the soil
5 solution of the organic-rich surface horizon at the beginning of storm events and of the
6 organic-poor deep horizon at the end of storm events. We separated the storm-flow
7 hydrograph into three successive components: (i) overland flow above the saturated wetland
8 soil horizons; (ii) subsurface flow through the uppermost organic-rich horizon of wetland
9 soils; and (iii) subsurface return flow from shallow hillslope groundwater passing through
10 deeper organic-poor soil horizons in wetlands (Lambert et al., 2011, 2014). These patterns
11 supported the hypothesis that a portion of DOM flux during storm is generated by
12 mobilization of pre-existing DOM pools during water table rise.

13 **2.3 Sampling**

14 Soils from the Mercy wetland were sampled with a hand auger in October 2010. Three sample
15 subsets were collected in the organo-mineral (0-10 cm) and the mineral (30-40 cm) horizons.
16 After removal of roots and gravels by hand, all samples were freeze-dried and crushed using
17 an agate mortar.

18 Five storm events were sampled between December 04, 2010 and February 19, 2011, during
19 hydrological period B, when wetland soils are most hydrologically connected to stream flow
20 (Figure 2). Numbering of storm events follows Lambert et al. (2014). Events 2, 3, 4, 5 and 6
21 were sampled on December 4, December 19, January 6, February 13 and February 19,
22 respectively. An automatic gauge station at the outlet of the catchment recorded stream
23 discharge every minute. The beginning of a flood was determined by an increase of the stream
24 discharge $> 1 \text{ L s}^{-1}$ over 10 minutes. Turbidity was monitored by a APC-TU Ponselle every 30
25 seconds, with 10 minute averages reorded. Cumulative rainfall was recorded every hour at a
26 weather station located ca. 300 m from the catchment outlet. An automatic sampler (Sigma
27 900 Max) collected 1 L stream water during storms which were stored at 4°C in
28 polypropylene (PP) bottles in a shed at the outlet of the catchment (Figure 1) and were stored
29 in polypropylene (PP) bottles. Sampling frequency during storm events varied from one
30 sample every 30 min to one sample every hour, depending on the hydrograph variations.
31 During baseflow conditionsbetween storms, we collected manual samples daily (5 p.m.) in 60

1 mL PP bottles for DOC monitoring and every two weeks in 1 L glass bottles for isotopic and molecular analyses. Stream water was filtered at 0.22 μm using cellulose acetate membrane filters pre-washed with 500 mL of de-ionized water and rinsed with a few mL of the sample itself. Filtered water samples were acidified using 1 N HCl (1 mL per L of sample) to remove inorganic carbon and then were frozen and freeze-dried.

2.4 Analytical procedure

We introduced approximately 2 mg of solid residue (soil or lyophilizate) into an 80 μL aluminum reactor with an excess of solid tetramethylammonium hydroxide (TMAH – ca. 10 mg). The THM reaction was performed on-line using a vertical micro-furnace pyrolyser PZ-2020D (Frontier Laboratories, Japan) operating at 400°C for 1 minute. The products of this reaction were injected into a gas chromatograph (GC) GC-2010 (Shimadzu, Japan) equipped with a SLB 5MS capillary column in the split mode (60 m \times 0.25 mm ID, 0.25 μm film thickness). The split ratio was adapted according to the sample and ranged from 15 to 30. The temperature of the transfer line was 321°C and the temperature of the injection port was 310°C. The oven was programmed to maintain an initial temperature of 50°C for 2 minutes, then rise to 150°C at 15°C min⁻¹, and then rise to 310°C at 3 °C min⁻¹ where it stayed for 14 minutes. Helium was used as the carrier gas, with a flow rate of 1.0 ml/min. Compounds were detected using a QP2010+ mass spectrometer (MS) (Shimadzu, Japan) operating in the full scan mode. The temperature of the transfer line was set at 280°C, the ionization source at 200°C, and molecules were ionized by electron impact using an energy of 70 eV. The list of analyzed compounds and m/z ratios used for their integration are given in the supplementary materials (Table S1). Compounds were identified on the basis of their full-scan mass spectra by comparison with the NIST library and with published data (Nierop et al., 2005; Nierop and Verstraten, 2004). They were classified into three categories: lignin and tannin (LIG-TAN) markers, carbohydrates (CAR) and fatty acids (FA). The peak area of the selected m/z for each compound was integrated and corrected by a mass spectra factor (MSF) calculated as the reciprocal of the proportion of the fragment used for the integration and the entire fragmentogram provided by the NIST library. The proportion of each compound class was calculated by dividing the sum of the areas of the compounds in this class by the sum of the peak areas of all analyzed compounds expressed as a percentage. Since no internal standards were used, data were interpreted qualitatively. Five samples were analyzed in triplicate to quantify reproducibility of the analysis. The relative standard deviation (RSD) calculated for

carbohydrate proxy, lignin-tannin proxies and the proportion of plant-derived markers was 9, 10 and 6%, respectively. The uncertainties given in Figures 3, 4, 5 and S1 correspond to these mean RSD values. The use of THM-GC-MS to investigate the temporal variability of the DOM composition meant that it was necessary to assume that the ionization efficiency and matrix effects are equivalent for all analyzed compounds in all samples.

2.5 Analysis of molecular data

We used two metrics to investigate the distribution of lignin-tannin markers produced by the THM reaction. First, we used the ratio of the sum of coumaric and ferulic acid to the sum of vanillic acid, vanillaldehyde and acetovanillone (C/V ratio). Second, we used the ratio of vanillic acid to vanillaldehyde (Ac/Al (V) ratio).

We classified molecular markers generated by THM-GC-MS into microbial and plant-derived markers as described by Jeanneau et al. (2014). Briefly, lignin-tannins were characteristic of DOM derived from plant sources whereas carbohydrates and fatty acids can come from both plant and microbial sources. The proportion of microbial carbohydrates was calculated using an end-member mixing approach (EMMA; Equation 1) based on the deoxyC6/C5 ratio, assuming 0.5 and 2.0 for plant-derived ($deoxyC6/C5_{plant}$) and microbial ($deoxyC6/C5_{mic}$) inputs, respectively (Rumpel and Dignac, 2006):

$$f_{mic}^{CAR} = \left(\frac{deoxyC6}{C5} - \frac{deoxyC6}{C5}_{plant} \right) \div \left(\frac{deoxyC6}{C5}_{mic} - \frac{deoxyC6}{C5}_{plant} \right) \quad (1)$$

C6 were not considered since they can derive from the THM of cellulose leading to an increase of the plant-derived C6 signal. The proportion of microbial fatty acids was calculated as the % low molecular weight fatty acids (< C19) by excluding C16:0 and C18:0, which can be derive from plant or microbial inputs. The microbial FA were composed of C12:0, C13:0, C14:0, C15:0, C17:0, *anteiso* and *iso* C15:0 and C17:0, *iso* C16:0, C16:1 and C18:1, which are commonly used as bacterial indicators (Frostegård et al., 1993). The fraction of microbial markers (f_{mic}) was calculated as the sum of the proportion of microbial CAR (f_{mic}^{CAR}) multiplied by the proportion of CAR ($\%_{CAR}$) plus the proportion of microbial FA (f_{mic}^{FA}) multiplied by the proportion of FA ($\%_{FA}$) (Equation 2):

$$f_{mic} = f_{mic}^{CAR} \times \%_{CAR} + f_{mic}^{FA} \times \%_{FA} \quad (2)$$

From this value, it is possible to calculate the proportion of plant-derived markers among the analyzed compounds (f_{plant}) (Equation 3):

$$f_{mic} + f_{plant} = 100 \quad (3)$$

For those calculations, we assume that the distribution of carbohydrates and fatty acids was conserved during transport, attributing all differences to the relative proportion of plant-derived and microbial inputs. Although these assumptions still need to be validated by investigating pure and known mixtures of vegetal and microbial sources, this approach can be used to approximate f_{mic} and f_{plant} .

3 Results

3.1 Soils and soil solution

Ratios of lignin-tannin composition were poorly associated with spatio-temporal variations of the composition of soil DOM in the Mercy wetland (Jeanneau et al., 2014). However they can differentiate stream DOM between inter-storm and storm conditions (Dalzell et al., 2005; Hernes et al., 2008) leading to the assumption of stream DOM produced by an erosive process. In SOM from the Mercy wetland, the C/V ratio was 1.3 and 1.6 in surface and deep horizons, respectively. The Ac/Al (V) ratio was 2.6 and 1.6 in surface and deep horizons, respectively. In soil DOM from November 29, 2010 to March 11, 2011, the C/V ratio ranged from 0.2 to 0.4 in the surface horizon and remained stable at 0.2 in the deep horizon. The Ac/Al (V) ratio ranged from 7.1 to 12.1 (9.1 ± 1.7 , mean \pm SD) in the surface horizon and from 3.6 to 6.9 (4.7 ± 1.2 , mean \pm SD) in the deep horizon.

3.2 River DOM in inter-storm conditions

In river samples from November 28, 2010 to March 8, 2011, f_{plant} ranged from 34 to 48% of all analyzed compounds (Figure 3). Among carbohydrates, the ratio deoxyC6/C5 ranged from 1.0 to 1.6 and heptoses have never been detected in those samples. For lignin-tannin, the C/V ratio remained lower than 0.2 with the exception of the sampling of January 7, 2011, which had a value of 0.5. The Ac/Al (V) ratio ranged from 4.5 to 7.7.

3.3 River DOM during storm events

During the five sampled storm events, the DOM composition showed shifts in isotopes (Lambert et al., 2014) and molecular markers analyses (Figures 4 and S1, Table 1). The modifications, displayed on Figure 4 for the events 3 and 4, were relatively consistent for the five storm events. During storm events, f_{plant} increased from an initial value of 31% (events 2, 4 and 6), 49% (event 3) and 14 % (event 5), reaching maximal values of 63% (event 6) to 82 % (event 3) during peak flow (Figure 4 and Table 1). After the peak flow, f_{plant} decreased by approximately 10 % (events 2, 4, 5 and 6) or remained stable (event 3) until the end of the sample collection.

Composition of carbohydrate, as reflected in the deoxyC6/C5 ratio, also varied during storm events, decreasing with discharge from initial values ranging from 1.5 to 2.7, and reaching its minimal value at peak flow and then remaining stable through the end of the sampling. Heptoses were detected in the first samples at the beginning of all storm events and up to the fifth sample for event 2 (Figure S2).

The C/V and Ac/Al (V) ratios, metrics of the composition of lignin-tannin were modified during storm events. The C/V ratio increased with discharge from 0.2 at the beginning of storm events to 0.5 (event 5), 0.6 (events 2 and 4), 0.7 (event 3) and 0.8 (event 6). Depending of the storm event, this value slightly decreased or remained stable through the end of the sampling. The evolution of the Ac/Al (V) ratio was storm-dependant. For events 2, 4 and 6, it remained stable around 5.0 with a few extreme values, while for the events 3 and 5, it decreased from 7.0 to 5.0 with the increase of the discharge and then remained stable through the end of the sampling.

4 Discussion

4.1 Inter-storm stream DOM

The f_{plant} of inter-storm stream DOM was composed of a mix of soil DOM from the organic-rich and organic-poor horizons (Figure 3). Since f_{plant} of soil DOM differed strongly between organo-mineral and mineral horizons and was fairly stable during the investigated period (Figure 3), it can be used in an end member mixing approach to determine the relative DOM contributions of organo-mineral and mineral horizons. From November 29, 2010 to

March 11, 2011 the proportion of stream DOM originating from organo-mineral horizon ranged from 23 to 59 % ($37 \pm 13\%$, mean \pm SE). This confirms previous findings that near-surface, organic-rich soils in riparian wetland zones are important DOM sources even during non-storm conditions (Strohmeier et al., 2013).

4.2 A pulse of microbial DOM at the beginning of storms

At the beginning of the storm events f_{plant} of stream DOM decreased, with the exception of event 3. The higher value recorded for event 3 was likely due to an increase in discharge the previous day (from 48 to 78 l s^{-1} ; Table S2), which could have mobilized microbial compounds before the first sampling. Stream DOM at beginning of storm events was also characterized by higher deoxyC6/C5 ratio than during inter-storm conditions and by the occurrence of heptoses. Heptoses have been detected in microbial exopolysaccharides (Jiao et al., 2010) and lipopolysaccharides (Sadovskaya et al., 1998). The export of microbial DOM, evidenced by the presence of heptoses and high f_{mic} was most prevalent for event 5 where 86% of the analyzed biomarkers were of microbial origin during the earliest stages of the storm. This was the first flood after the onset of reducing conditions in wetland soils (Lambert et al., 2013), when the riparian wetland zones at the soil-river interface were a hotspot of iron reduction.

This pool of microbial DOM could derive from a flushing of microbial lysis products accumulated in soils over the dry period (Christ and David, 1996). However, the five sampled storm events occurred during the hydrological phase B, where riparian wetland soils are continuously waterlogged, precluding the possibility of lysis from dessication. Moreover, heptoses were not detected in soil DOM or in stream DOM samples during inter-storm conditions. Alternatively, microbially-derived DOM could come from microbial biofilms in soil macropores or at the wetland-stream interface (Knorr, 2013), that are destabilized and transported into the stream by the increase of water velocity at the beginning of storm events (Trulear and Characklis, 1982). Regardless the mechanism, this pulse of microbial DOM at the beginning of storm events could account for the compositional shift in stream DOM observed with high-frequency fluorescence measurements and displayed in the literature. Indeed soil DOM of the first storm samples is often characterized by high proportions of protein-like chromophores, low proportions of humic-like chromophores (Knorr, 2013), high fluorescence index, and low SUVA (Inamdar et al., 2011; Vidon et al., 2008).

4.3 Soil erosion as a DOM producer

Storm events caused a shift in the compositional ratios of lignin-tannin. The C/V ratio increased from 0.2 to 0.8 and the Ac/Al (V) ratio decreased from 7 to 5 with the exception of event 6 where it remained stable around 5. These modifications of lignin-tannin transfer from soils to rivers during flood events are in accordance with data on lignin phenols obtained along the Big Pine Creek watershed (Dalzell et al., 2005) and the Willow Slough watershed (Hernes et al., 2008). In both of those watersheds, stream DOM during storms was characterized by higher C/V and lower Ac/Al (V) ratios than DOM sampled during inter-storm conditions. Although the differences in analytical techniques makes direct data comparison difficult (Wysocki et al., 2008), the compositional ratios show the same pattern during biodegradation with a decrease in the C/V ratio and an increase in the Ac/Al (V) ratio (Kabuyah et al., 2012; Vane et al., 2005). The aforementioned modifications of C/V and Ac/Al (V) ratios have consequently been attributed to the mobilization of less-degraded lignins during flood events (Dalzell et al., 2005; Hernes et al., 2008).

In soils, the partitioning of OM between the particulate phase (SOM) and the soil solution (soil DOM) occurs continuously with a high soil/water ratio producing soil DOM characterized by low C/V (around 0.2). During storm events, the values of the C/V ratio in stream DOM increased to values higher than those recorded in the soil solutions. Thus stream DOM during storms cannot only result from the passive transfer of pre-existing soil DOM to the stream. Of all the known DOM sources in the catchment, only SOM has C/V values that could explain the elevated storm DOM values (Figure 5). In the Willow Slough catchment, the concentration in lignin markers is correlated with the concentration of suspended matter indicating that a portion of DOM during storm events can be inherited from the partitioning of organic compounds between solid and dissolved phases (Hernes et al., 2008). Lignin-tannin and suspended sediment were also correlated in the present study, as seen in the regression between turbidity and C/V ratio (Figure 6). During storm event, erosion carries particles in water. These low soil/water conditions could induce a displacement of the equilibrium between OM in the solid phase and OM in the dissolved phase, which would lead to DOM with a high C/V (higher or equal to 0.8). Soil erosion and the equilibrium between solid (soil particles) and dissolved (river) phases is likely an additional source of DOM transfer from soil to rivers during storm events.

However, the positive relationship between turbidity and C/V ratio occurs primarily during the rising limb of the hydrograph (grey square, $R^2 = 0.68$, p -value < 0.0001 , $n = 23$), whereas after peak discharge, turbidity decreased while the C/V ratio remained high leading to a weaker correlation when all the samples are considered (black square, $R^2 = 0.11$, p -value $= 0.008$, $n = 64$). The persistence of high C/V ratios during the falling limb of the hydrograph highlights how other DOM production mechanisms inducing low soil/water conditions are also active during storms in addition to soil erosion. This could come from the exposure of new surfaces within soil structure following destabilization and the disaggregation of soil aggregates during the erosion of macropores walls during storm flow (Wilson et al., 2005). Such a mechanism could modify DOM production in soil profile, causing a shift in DOM composition persisting past peak flow, without adding suspended solid in the stream, the latter particles being physically trapped by the soil matrix.

4.4 Temporal scheme of DOM producing processes during storm events

Divergent behavior in the response of DOM concentration and composition to storms as we observed here has been documented in other catchments in various climates, with modifications to DOM composition typically persisting after concentration has returned to pre-event levels (Austnes et al., 2010; Knorr, 2013; Singh et al., 2015). This suggests that the mechanisms controlling DOM transport during different hydrologic conditions are general. Our work, in combination with previous results suggests a succession of four distinct mechanisms. First, between storms, DOM comes from the flushing of wetland soils horizons without major compositional changes of DOM during transport. The water table level would determine the contribution of organo-mineral and mineral soil horizons during this period. Second, at the beginning of rain events, the increase in water velocity could induce the destabilization of microbial biofilms, resulting in the release of a pulse of microbially-derived DOM. Third, the rise of the water table, in association with the decrease of lateral hydraulic conductivity with depth (Seibert et al., 2009) would increase the proportion of the water flowing through the upper, organic-rich surface horizon in the wetland, causing an increase of the stream DOC concentration. At the same time, erosion of soils and riverbanks would increase turbidity, leading to a partition of organic matter between particles and dissolved phase. The magnitude of the effect of this soil surface erosive process on DOM chemistry would depend on the concentration of suspended matter and would therefore decrease during the falling limb of the hydrograph. Finally, the increase in water velocity in soils could erode

macropore walls in the soil profile, leading to an in-soil partitioning between soil microparticles and dissolved phase. The contribution of this in-soil erosive process would be linked to the magnitude of the hydraulic gradient following the rise of water table. Since the return to pre-event conditions takes longer in the soil profile than for discharge (Lambert et al., 2014 – Fig 3.b), this could explain why compositional proxies of DOM do not recover as quickly as stream DOC concentrations. High-frequency sampling of soil solutions during and after storm events until return to pre-event values would be necessary to test these proposed mechanisms.

4.5 Summary and implications

We observed striking changes in DOM sources and transfer processes during and between storm events. While DOM during inter-storm conditions appears to be derived from the passive transfer of DOM from riparian wetland soils, during storm periods the DOM transferred from soil to the stream was not only due to flushing of DOM already present in soils but also to additional sources and production processes that increase the proportion of less-degraded molecules in the dissolved phase. Based on the current literature, these findings appear to quite general of DOM transfer in lowland catchments worldwide and have two important implications.

First, these results enhance our understanding of the transfer of micropollutants, which is largely controlled by the complexing properties of OM. The leaching of DOM from SOM during storm events increased the prevalence of less-biodegraded but more hydrophobic molecules (Kleber and Johnson, 2010). SOM hydrophobicity is believed to be the main driving force of the retention of hydrophobic micropollutants in soils, such as many pesticides and antibiotics (Ji et al., 2011). Increases in less-biodegraded, hydrophobic DOM during storms could therefore lead to enhanced transfer of these harmful compounds from soils to streams, increasing their bioavailability and consequently their undesirable effects, such as antibiotic resistance (Hellweger et al., 2011).

Secondly, our work has implications for modeling DOM export in headwater catchments. In lowland headwater catchments, up to 80% of DOM is transferred during storm events (Raymond and Saiers, 2010), and many modeling studies assume that DOM transfer during storm events consists of the flushing of pre-existing soil pools. Since these soil DOM pools are calibrated for concentration and composition using samples taken in inter-storm

conditions, these models don't account for alternative DOM producing processes activated during storms, such as the surface and subsurface erosion processes proposed here. This oversight could explain why modeling studies succeed in reproducing inter-storm DOM concentrations, but not storm flow DOM dynamics (Birkel et al., 2014). Increased interaction between geochemists and modelers could accelerate the conceptualization of temporally and spatially variant DOM production mechanisms and improve modeling of DOM export.

Acknowledgements

We thank the technical staff from INRA and Géosciences Rennes for their assistance during the fieldwork. This research was funded by the University of Rennes 1 through the “Variamod” project and by the CNRS through the EC2CO “Prodynamos” project. We used data provided online by the environmental observatory ORE AgrHys (www6.inra.fr/ore_agrhys_eng/). The authors thank Dr B.W. Abbott who copy-edited the manuscript for the use of English.

References

- Ågren, A., Buffam, I., Jansson, M. and Laudon, H.: Importance of seasonality and small streams for the landscape regulation of dissolved organic carbon export, *J. Geophys. Res. Biogeosciences*, 112(G3), G03003, 2007.
- Aubert, A. H., Gascuel-Oudou, C., Gruau, G., Akkal, N., Fauchoux, M., Fauvel, Y., Grimaldi, C., Hamon, Y., Jaffrézic, A., Lecoz-Boutnik, M., Molénat, J., Petitjean, P., Ruiz, L. and Merot, P.: Solute transport dynamics in small, shallow groundwater-dominated agricultural catchments: insights from a high-frequency, multisolute 10 yr-long monitoring study, *Hydrol Earth Syst Sci*, 17(4), 1379–1391, 2013.
- Austnes, K., Evans, C., Eliot-Laize, C., Naden, P. and Old, G.: Effects of storm events on mobilisation and in-stream processing of dissolved organic matter (DOM) in a Welsh peatland catchment, *Biogeochemistry*, 99(1-3), 157–173, 2010.
- Billett, M. F., Deacon, C. M., Palmer, S. M., Dawson, J. J. C. and Hope, D.: Connecting organic carbon in stream water and soils in a peatland catchment, *J. Geophys. Res. Biogeosciences*, 111(G2), G02010, 2006.
- Birkel, C., Soulsby, C. and Tetzlaff, D.: Integrating parsimonious models of hydrological connectivity and soil biogeochemistry to simulate stream DOC dynamics, *J. Geophys. Res. Biogeosciences*, 119(5), 2013JG002551, 2014.
- Bishop, K., Buffam, I., Erlandsson, M., Fölster, J., Laudon, H., Seibert, J. and Temnerud, J.: Aqua Incognita: the unknown headwaters, *Hydrol. Process.*, 22(8), 1239–1242, 2008.

- 1 Christ, M. J. and David, M. B.: Temperature and moisture effects on the production of
2 dissolved organic carbon in a Spodosol, *Soil Biol. Biochem.*, 28(9), 1191–1199, 1996.
- 3 Cole, J. J., Prairie, Y. T., Caraco, N. F., McDowell, W. H., Tranvik, L. J., Striegl, R. G.,
4 Duarte, C. M., Kortelainen, P., Downing, J. A., Middelburg, J. J. and Melack, J.: Plumbing
5 the Global Carbon Cycle: Integrating Inland Waters into the Terrestrial Carbon Budget,
6 *Ecosystems*, 10(1), 172–185, 2007.
- 7 Corapcioglu, M. Y. and Jiang, S.: Colloid-facilitated groundwater contaminant transport,
8 *Water Resour. Res.*, 29(7), 2215–2226, 1993.
- 9 Cranwell, P. A.: Monocarboxylic acids in lake sediments: Indicators, derived from terrestrial
10 and aquatic biota, of paleoenvironmental trophic levels, *Chem. Geol.*, 14(1–2), 1–14, 1974.
- 11 Crave, A. and Gascuel-Oudou, C.: The influence of topography on time and space distribution
12 of soil surface water content, *Hydrol. Process.*, 11(2), 203–210, 1997.
- 13 Dalzell, B. J., Filley, T. R. and Harbor, J. M.: Flood pulse influences on terrestrial organic
14 matter export from an agricultural watershed, *J Geophys Res*, 110(G2), G02011, 2005.
- 15 Durand, P. and Juan Torres, J. L.: Solute transfer in agricultural catchments: the interest and
16 limits of mixing models, *J. Hydrol.*, 181(1–4), 1–22, 1996.
- 17 Eglinton, G. and Hamilton, R. J.: Leaf epicuticular waxes, *Science*, 156(3780), 1322–1335,
18 1967.
- 19 Frostegård, Å., Tunlid, A. and Bååth, E.: Phospholipid Fatty Acid Composition, Biomass, and
20 Activity of Microbial Communities from Two Soil Types Experimentally Exposed to
21 Different Heavy Metals, *Appl. Environ. Microbiol.*, 59(11), 3605–3617, 1993.
- 22 Grasset, L., Rovira, P. and Amblès, A.: TMAH-preparative thermochemolysis for the
23 characterization of organic matter in densimetric fractions of a Mediterranean forest soil, *J.*
24 *Anal. Appl. Pyrolysis*, 85(1-2), 435–441, 2009.
- 25 Hedges, J. I. and Parker, P. L.: Land-derived organic matter in surface sediments from the
26 Gulf of Mexico, *Geochim. Cosmochim. Acta*, 40(9), 1019–1029, 1976.
- 27 Hellweger, F. L., Ruan, X. and Sanchez, S.: A Simple Model of Tetracycline Antibiotic
28 Resistance in the Aquatic Environment (with Application to the Poudre River), *Int. J.*
29 *Environ. Res. Public. Health*, 8(2), 480–497, 2011.
- 30 Hernes, P. J., Spencer, R. G. M., Dyda, R. Y., Pellerin, B. A., Bachand, P. A. M. and
31 Bergamaschi, B. A.: The role of hydrologic regimes on dissolved organic carbon composition
32 in an agricultural watershed, *Geochim. Cosmochim. Acta*, 72(21), 5266–5277, 2008.
- 33 Hinton, M. J., Schiff, S. L. and English, M. C.: Sources and flowpaths of dissolved organic
34 carbon during storms in two forested watersheds of the Precambrian Shield, *Biogeochemistry*,
35 41(2), 175–197, 1998.

- 1 Hood, E., Gooseff, M. N. and Johnson, S. L.: Changes in the character of stream water
2 dissolved organic carbon during flushing in three small watersheds, Oregon, *J Geophys Res*,
3 111(G1), G01007, 2006.
- 4 Inamdar, S., Singh, S., Dutta, S., Levia, D., Mitchell, M., Scott, D., Bais, H. and McHale, P.:
5 Fluorescence characteristics and sources of dissolved organic matter for stream water during
6 storm events in a forested mid-Atlantic watershed, *J Geophys Res*, 116(G3), G03043, 2011.
- 7 IUSS Working Group WRB: World reference base for soil resources 2006, World Soil
8 Resources Reports No. 103. FAO, Rome, 2006.
- 9 Jeanneau, L., Jaffrezic, A., Pierson-Wickmann, A.-C., Gruau, G., Lambert, T. and Petitjean,
10 P.: Constraints on the Sources and Production Mechanisms of Dissolved Organic Matter in
11 Soils from Molecular Biomarkers, *Vadose Zone J.*, 13(7), 2014.
- 12 Jiao, Y., Cody, G. D., Harding, A. K., Wilmes, P., Schrenk, M., Wheeler, K. E., Banfield, J.
13 F. and Thelen, M. P.: Characterization of Extracellular Polymeric Substances from
14 Acidophilic Microbial Biofilms, *Appl. Environ. Microbiol.*, 76(9), 2916–2922, 2010.
- 15 Ji, L., Wan, Y., Zheng, S. and Zhu, D.: Adsorption of Tetracycline and Sulfamethoxazole on
16 Crop Residue-Derived Ashes: Implication for the Relative Importance of Black Carbon to
17 Soil Sorption, *Environ. Sci. Technol.*, 45(13), 5580–5586, 2011.
- 18 Kabuyah, R. N. T. M., van Dongen, B. E., Bewsher, A. D. and Robinson, C. H.:
19 Decomposition of lignin in wheat straw in a sand-dune grassland, *Soil Biol. Biochem.*, 45(0),
20 128–131, 2012.
- 21 Kicklighter, D. W., Hayes, D. J., McClelland, J. W., Peterson, B. J., McGuire, A. D. and
22 Melillo, J. M.: Insights and issues with simulating terrestrial DOC loading of Arctic river
23 networks, *Ecol. Appl.*, 23(8), 1817–1836, 2013.
- 24 Kleber, M. and Johnson, M. G.: Advances in Understanding the Molecular Structure of Soil
25 Organic Matter: Implications for Interactions in the Environment, *Advances in Agronomy*,
26 106, 77–142, 2010.
- 27 Knorr, K.-H.: DOC-dynamics in a small headwater catchment as driven by redox fluctuations
28 and hydrological flow paths – are DOC exports mediated by iron reduction/oxidation cycles?,
29 *Biogeosciences*, 10(2), 891–904, 2013.
- 30 Lambert, T., Pierson-Wickmann, A.-C., Gruau, G., Thibault, J.-N. and Jaffrezic, A.: Carbon
31 isotopes as tracers of dissolved organic carbon sources and water pathways in headwater
32 catchments, *J. Hydrol.*, 402(3–4), 228–238, 2011.
- 33 Lambert, T., Pierson-Wickmann, A.-C., Gruau, G., Jaffrezic, A., Petitjean, P., Thibault, J.-N.
34 and Jeanneau, L.: Hydrologically driven seasonal changes in the sources and production
35 mechanisms of dissolved organic carbon in a small lowland catchment, *Water Resour. Res.*,
36 49, 1–12, 2013.
- 37 Lambert, T., Pierson-Wickmann, A.-C., Gruau, G., Jaffrezic, A., Petitjean, P., Thibault, J. N.
38 and Jeanneau, L.: DOC sources and DOC transport pathways in a small headwater catchment

- 1 as revealed by carbon isotope fluctuation during storm events, *Biogeosciences*, 11(11), 3043–
2 3056, 2014.
- 3 Lucas García, J. A., Barbas, C., Probanza, A., Barrientos, M. L. and Gutierrez Mañero, F. J.:
4 Low molecular weight organic acids and fatty acids in root exudates of two *Lupinus* cultivars
5 at flowering and fruiting stages, *Phytochem. Anal.*, 12(5), 305–311, 2001.
- 6 Matsuda, H. and Koyama, T.: Early diagenesis of fatty acids in lacustrine sediments—II. A
7 statistical approach to changes in fatty acid composition from recent sediments and some
8 source materials, *Geochim. Cosmochim. Acta*, 41(12), 1825–1834, 1977.
- 9 Maurice, P. A., Cabaniss, S. E., Drummond, J. and Ito, E.: Hydrogeochemical controls on the
10 variations in chemical characteristics of natural organic matter at a small freshwater wetland,
11 *Chem. Geol.*, 187(1–2), 59–77, 2002.
- 12 McDonnell, J. J.: Where does water go when it rains? Moving beyond the variable source area
13 concept of rainfall-runoff response, *Hydrol. Process.*, 17(9), 1869–1875, 2003.
- 14 McGlynn, B. L. and McDonnell, J. J.: Role of discrete landscape units in controlling
15 catchment dissolved organic carbon dynamics, *Water Resour Res.*, 39(4), 1090, 2003.
- 16 McLaughlin, C. and Kaplan, L. A.: Biological lability of dissolved organic carbon in stream
17 water and contributing terrestrial sources, *Freshw. Sci.*, 32(4), 1219–1230, 2013.
- 18 Molenat, J., Gascuel-Oudou, C., Ruiz, L. and Gruau, G.: Role of water table dynamics on
19 stream nitrate export and concentration in agricultural headwater catchment (France), *J.*
20 *Hydrol.*, 348(3–4), 363–378, 2008.
- 21 Morel, B., Durand, P., Jaffrezic, A., Gruau, G. and Molenat, J.: Sources of dissolved organic
22 carbon during stormflow in a headwater agricultural catchment, *Hydrol. Process.*, 23(20),
23 2888–2901, 2009.
- 24 Nierop, K. G. J. and Verstraten, J. M.: Rapid molecular assessment of the bioturbation extent
25 in sandy soil horizons under pine using ester-bound lipids by on-line thermally assisted
26 hydrolysis and methylation-gas chromatography/mass spectrometry, *Rapid Commun. Mass*
27 *Spectrom.*, 18(10), 1081–1088, 2004.
- 28 Nierop, K. G. J., Preston, C. M. and Kaal, J.: Thermally Assisted Hydrolysis and Methylation
29 of Purified Tannins from Plants, *Anal. Chem.*, 77(17), 5604–5614, 2005.
- 30 Raymond, P. and Saiers, J.: Event controlled DOC export from forested watersheds,
31 *Biogeochemistry*, 100(1-3), 197–209, 2010.
- 32 Raymond, P. A., Hartmann, J., Lauerwald, R., Sobek, S., McDonald, C., Hoover, M.,
33 Butman, D., Striegl, R., Mayorga, E., Humborg, C., Kortelainen, P., Durr, H., Meybeck, M.,
34 Ciais, P. and Guth, P.: Global carbon dioxide emissions from inland waters, *Nature*,
35 503(7476), 355–359, 2013.
- 36 Rumpel, C. and Dignac, M.-F.: Gas chromatographic analysis of monosaccharides in a forest
37 soil profile: Analysis by gas chromatography after trifluoroacetic acid hydrolysis and
38 reduction–acetylation, *Soil Biol. Biochem.*, 38(6), 1478–1481, 2006.

- 1 Sadvovskaya, I., Brisson, J.-R., Lam, J. S., Richards, J. C. and Altman, E.: Structural
2 elucidation of the lipopolysaccharide core regions of the wild-type strain PAO1 and O-chain-
3 deficient mutant strains AK1401 and AK1012 from *Pseudomonas aeruginosa* serotype O5,
4 *Eur. J. Biochem.*, 255(3), 673–684, 1998.
- 5 Saraceno, J. F., Pellerin, B. A., Downing, B. D., Boss, E., Bachand, P. A. M. and
6 Bergamaschi, B. A.: High-frequency in situ optical measurements during a storm event:
7 Assessing relationships between dissolved organic matter, sediment concentrations, and
8 hydrologic processes, *J Geophys Res*, 114, G00F09, 2009.
- 9 Seibert, J., Grabs, T., Köhler, S., Laudon, H., Winterdahl, M. and Bishop, K.: Linking soil-
10 and stream-water chemistry based on a Riparian Flow-Concentration Integration Model,
11 *Hydrol Earth Syst Sci*, 13(12), 2287–2297, 2009.
- 12 Singh, S., Inamdar, S. and Mitchell, M.: Changes in dissolved organic matter (DOM) amount
13 and composition along nested headwater stream locations during baseflow and stormflow,
14 *Hydrol. Process.*, 29(6), 1505–1520, 2015.
- 15 Strohmeier, S., Knorr, K.-H., Reichert, M., Frei, S., Fleckenstein, J. H., Peiffer, S. and
16 Matzner, E.: Concentrations and fluxes of dissolved organic carbon in runoff from a forested
17 catchment: insights from high frequency measurements, *Biogeosciences*, 10(2), 905–916,
18 2013.
- 19 Trulear, M. G. and Characklis, W. G.: Dynamics of biofilm processes, *J. Water Pollut.*
20 *Control Fed.*, 54(9), 1288–1301, 1982.
- 21 Vane, C. H., Drage, T. C., Snape, C. E., Stephenson, M. H. and Foster, C.: Decay of
22 cultivated apricot wood (*Prunus armeniaca*) by the ascomycete *Hypocrea sulphurea*, using
23 solid state ¹³C NMR and off-line TMAH thermochemolysis with GC–MS, *Int. Biodeterior.*
24 *Biodegrad.*, 55(3), 175–185, 2005.
- 25 Vidon, P., Wagner, L. and Soyeux, E.: Changes in the character of DOC in streams during
26 storms in two Midwestern watersheds with contrasting land uses, *Biogeochemistry*, 88(3),
27 257–270–270, 2008.
- 28 Wilson, G. V., Xu, M., Chen, Y., Liu, G. and Römkens, M. J. M.: Macropore flow and mass
29 wasting of gullies in the Loess Plateau, China, *Int. J. Sediment Res.*, 20(3), 249–258, 2005.
- 30 Wysocki, L. A., Filley, T. R. and Bianchi, T. S.: Comparison of two methods for the analysis
31 of lignin in marine sediments: CuO oxidation versus tetramethylammonium hydroxide
32 (TMAH) thermochemolysis, *Org. Geochem.*, 39(10), 1454–1461, 2008.
- 33 Yang, L., Guo, W., Chen, N., Hong, H., Huang, J., Xu, J. and Huang, S.: Influence of a
34 summer storm event on the flux and composition of dissolved organic matter in a subtropical
35 river, China, *Appl. Geochem.*, 28(0), 164–171, 2013.

36

Table 1. Changes in discharge, DOC concentration and metrics of DOM composition during storm events. Values are given for the first, peak discharge, and final samples.

Event		2	3	4	5	6
Date		Dec 4, 2010	Dec 19, 2010	Jan 6, 2011	Feb 13, 2011	Feb 19, 2011
Discharge (L s ⁻¹)	beg. ^a	79.8	88.8	59.1	72.8	77.7
	max. ^b	177.3	453.1	169.8	167.3	245.1
	end	127.4	113.1	104.0	96.2	102.5
DOC (mg L ⁻¹)	beg. ^a	7.4	6.6	6.4	7.4	8
	max. ^b	11.6	12.4	11.5	12.8	15.5
	end	9.8	7.4	8.0	11	9.1
<i>f_{plant}</i> (%)	beg. ^a	31	49	31	14	31
	max. ^b	67	78	70	71	59
	end	57	72	58	60	25
deoxyC6/C5	beg. ^a	1.6	1.5	1.6	2.7	1.9
	max. ^b	0.9	1.1	1.0	1.1	1.3
	end	1.1	1.1	0.9	1.2	1.4
C/V	beg. ^a	0.2	0.2	0.2	0.2	0.3
	max. ^b	0.4	0.6	0.6	0.4	0.8
	end	0.5	0.5	0.4	0.4	0.3
Ac/AI (V)	beg. ^a	5.0	7.3	5.5	6.6	5.2
	max. ^b	5.2	5.3	4.6	5.5	4.5
	end	4.7	4.9	4.3	4.8	4.6

^a Value recorded at the beginning of storm events.

^b Value recorded at the peak discharge.

1 **Figure captions**

2 Figure 1. Map of the Kervidy-Naizin critical zone observatory (Brittany, France). Grey areas
3 located along the channel network indicate the maximum extent of the wetland zones.
4 Coordinates of the outlet are 48.0057 North, 2.8313 East (decimal degrees).

5 Figure 2. Discharge (white area), daily rainfall (black area) and water table level in the
6 wetland domain (dashed line) during the hydrologic year 2010-2011. Sampled storm events
7 are indicated by numbers and arrows.

8 Figure 3. Variation of the molecular composition of inter-storm DOM in stream (C/V,
9 deoxyC6/C5 and f_{plant}). The grey area is delimited by the f_{plant} in soil DOM from the
10 organo-mineral and mineral horizons.

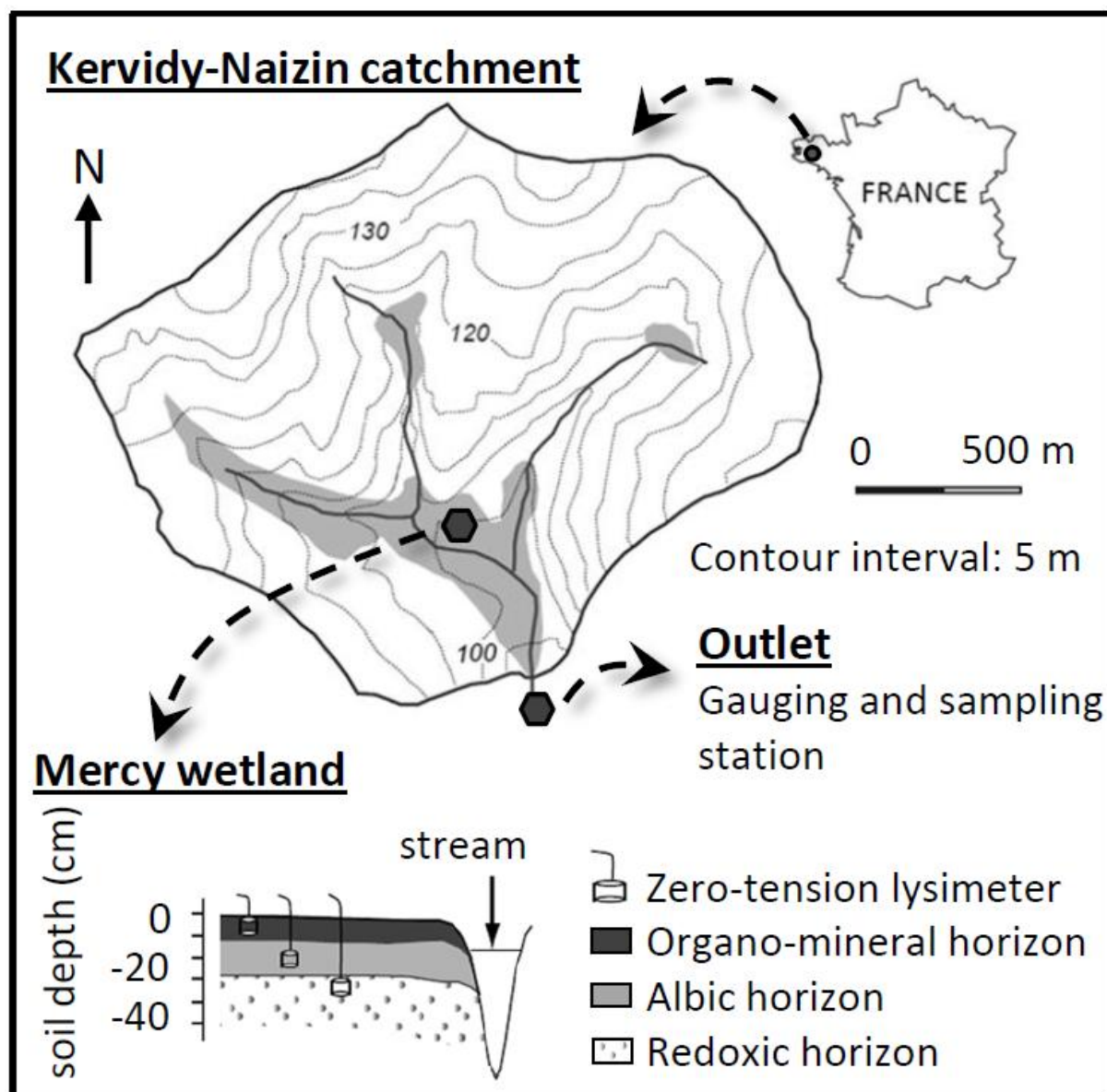
11 Figure 4. Temporal change in flow and DOC concentration and composition during storm
12 events 3 and 4. Various units indicated in the axis labels. The uncertainties for deoxyC6/C5,
13 f_{plant} , C/V and Ac/Al (V) are the mean RSD calculated for five samples analyzed in
14 triplicate.

15 Figure 5. Variation of the C/V ratio (lignin proxy) in SOM, soil DOM from organo-mineral
16 and mineral horizons, and stream DOM sampled during inter-storm and storm conditions.

17 Figure 6. Correlation between turbidity and the C/V ratio (lignin proxy) during the rising
18 limbs (grey diamonds – p -value < 0.0001) and during entire storm events (grey and black
19 diamonds – p -value = 0.008).

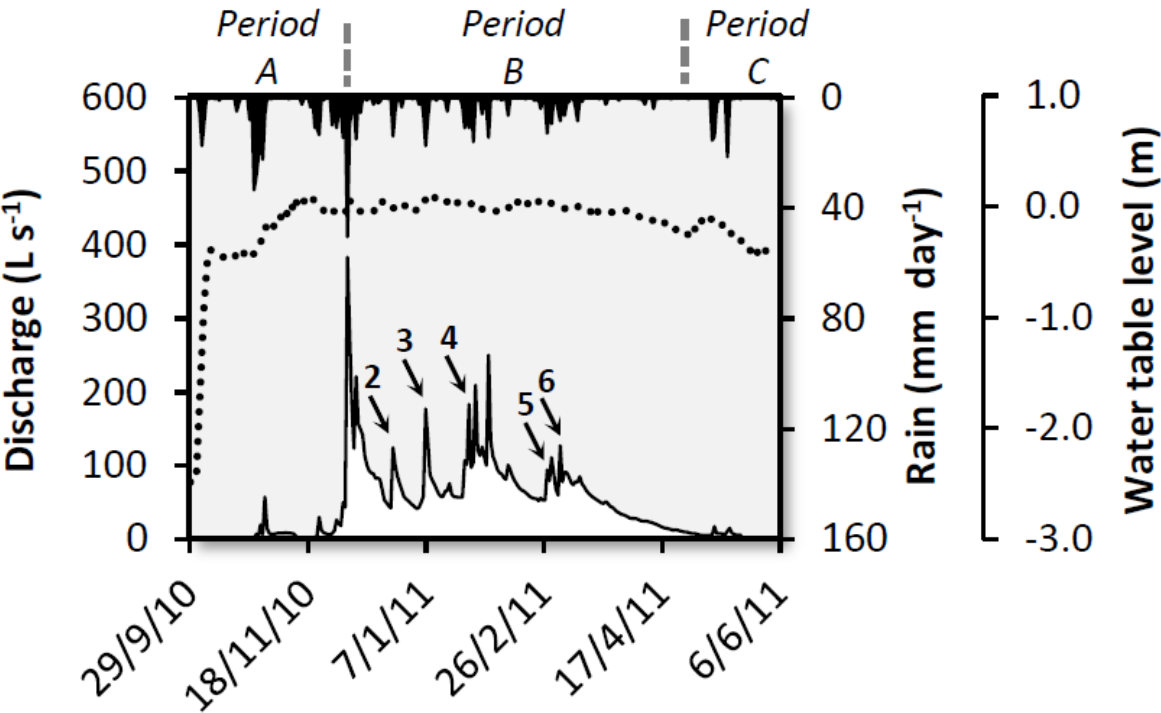
20

1 Figure 1



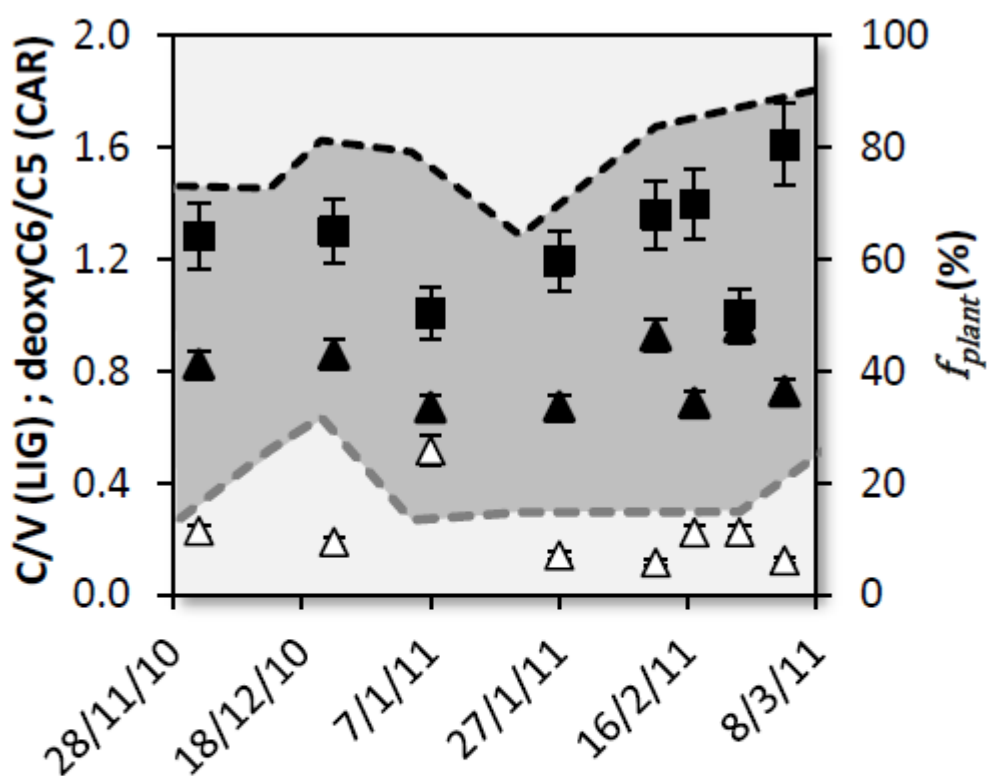
2
3

1 Figure 2



2
3

1 Figure 3



Caption:

Inter-storm stream DOM

■ deoxyC6/C5

△ C/V

▲ f_{plant}

Soil DOM: f_{plant}

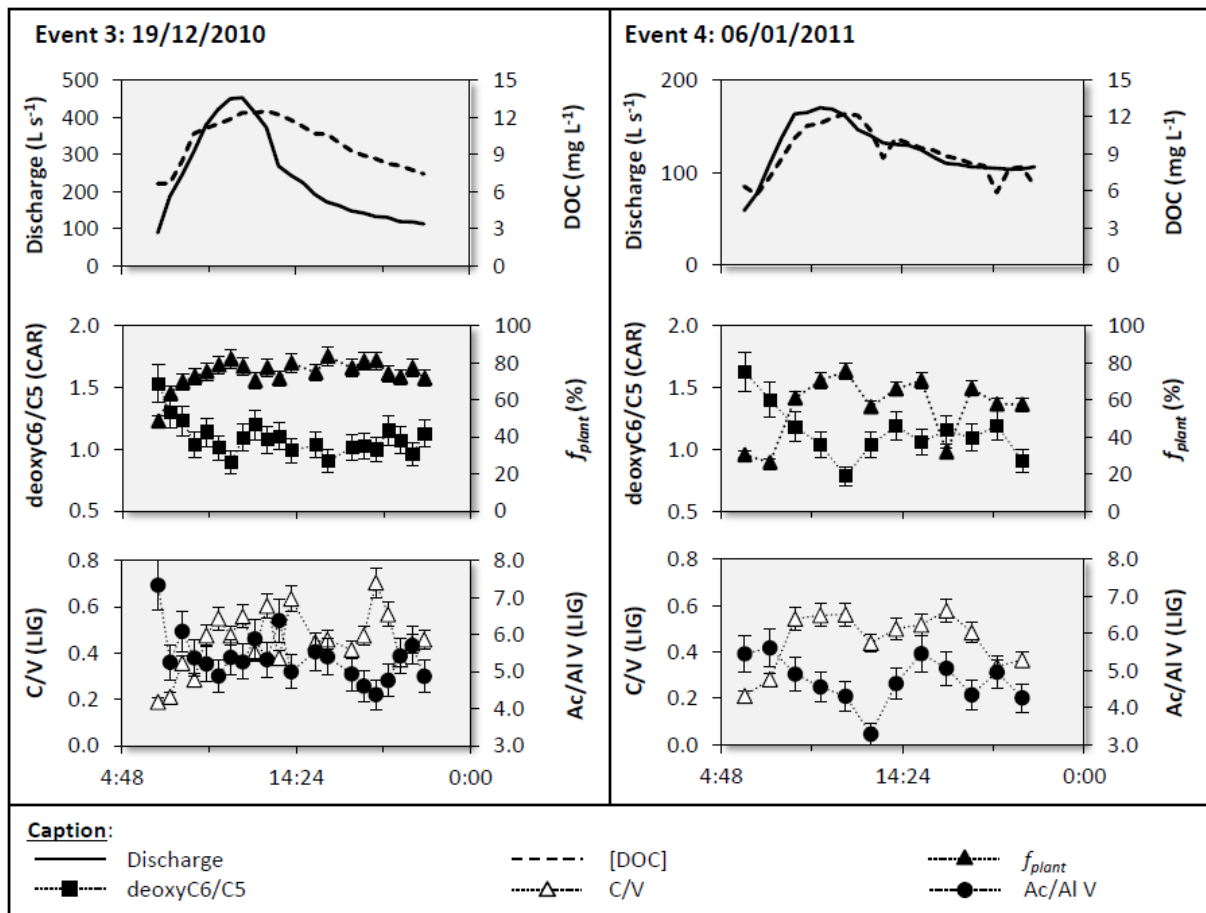
--- Organo-mineral horizon

--- Mineral horizon

2

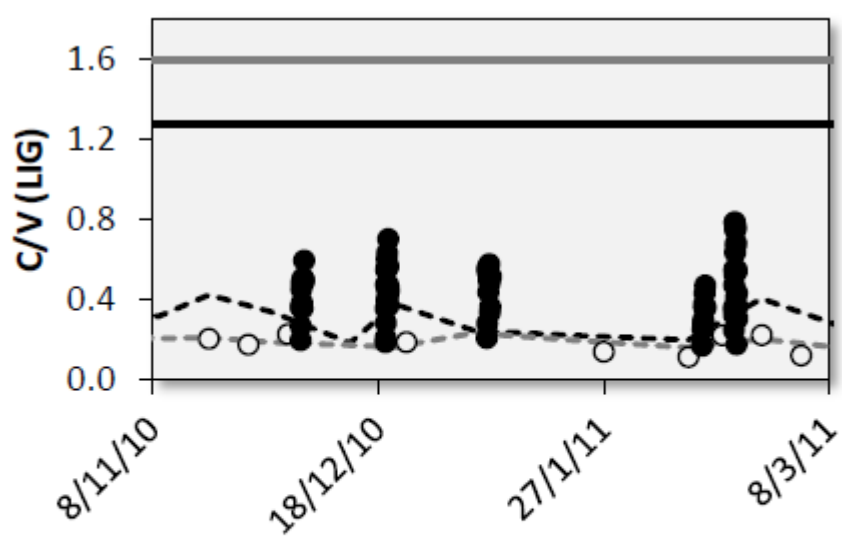
3

1 Figure 4



2
3

1 Figure 5



Caption:

SOM: — OM layer; — M layer

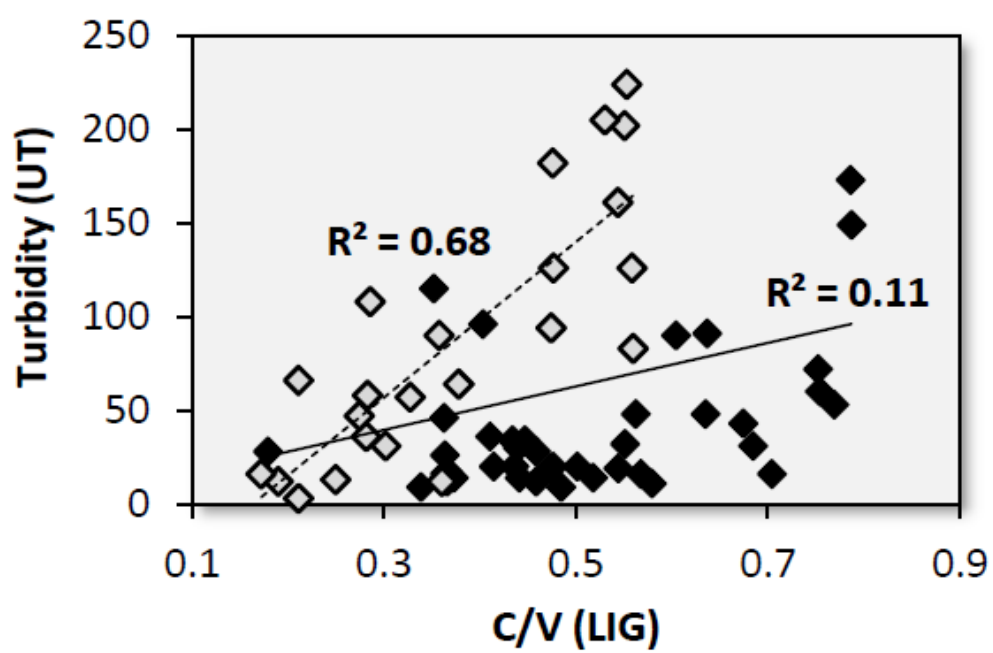
Soil DOM: - - - OM layer; - - - M layer

Stream DOM: ○ inter-storm; ● storm

2

3

1 Figure 6



Caption:

◆ Rising limb ◆ Entire event

2

3